Monomorphic epitheliotropic intestinal T-cell lymphoma comprises morphologic and genomic heterogeneity impacting outcome.

L. Veloza, Doriane Cavalieri, E. Missiaglia, Albane Ledoux-Pilon, B. Bisig, Bruno Pereira, C. Bonnet, Elsa Poullot, L. Quintanilla-Martinez, Romain Dubois, et al.

Monomorphic epitheliotropic intestinal T-cell lymphoma comprises morphologic and genomic heterogeneity impacting outcome

Luis Veloza,[1*] Doriane Cavalieri,[2*] Edoardo Missiaglia,[1] Albane Ledoux-Pilon,[3] Bettina Bisig,[1] Bruno Pereira,[4] Christophe Bonnet,[5] Elsa Poullot,[6] Leticia Quintanilla-Martinez,[7] Romain Dubois,[8] Francisco Llamas-Gutierrez,[9] Céline Bossard,[10] Roland De Wind,[11] Fanny Drieux,[12] Juliette Fontaine,[13] Marie Parrens,[14] Jeremy Sandrini,[15] Virginie Fataccioli,[6,16] Marie-Hélène Delfau-Larue,[16,17] Adrien Daniel,[18] Faustine Lhomme,[19] Lauriane Clément-Filliatre,[20] François Lemonnier,[16,21] Anne Cairoli,[22] Pierre Morel,[23] Sylvie Glaisner,[24] Bertrand Joly,[25] Abderrazak El Yamani,[26] Kamel Laribi,[27] Emmanuel Bachy,[28] Reiner Siebert,[29] David Vallois,[1] Philippe Gaulard,[6,16#] Olivier Tournilhac[2#] and Laurence de Leval[1#]

[1]Institute of Pathology, Department of Laboratory Medicine and Pathology, Lausanne University Hospital and Lausanne University, Lausanne, Switzerland; [2]Department of Hematology, University Hospital of Clermont-Ferrand, EA7453 CIC1405, Université Clermont Auvergne, Clermont-Ferrand, France; [3]Department of Pathology, University Hospital of Clermont-Ferrand, Clermont-Ferrand, France; [4]Clinical Research Direction, University Hospital of Clermont-Ferrand, Clermont-Ferrand, France; [5]Department of Hematology, University Hospital Sart Tilman, Liège, Belgium; [6]AP-HP, Henri Mondor Hospital, Pathology Department, Créteil, France; [7]Institute of Pathology, University Hospital Tübingen, Eberhard Karls University of Tübingen, Tübingen, Germany; [8]Department of Pathology, University Hospital of Lille, Lille, France; [9]Department of Pathology, University Center Hospital, Rennes, France; [10]Department of Pathology, CHU de Nantes, Nantes, France; [11]Department of Pathology, Institute Jules Bordet, Bruxelles, Belgique; [12]Service of Anatomical and Cytological Pathology, Center Henri Becquerel, Rouen, France; [13]Multisite Pathology Institute, Hôpital Lyon Sud, Hospices Civils de Lyon, Pierre Bénite, France; [14]Department of Pathology, CHU de Bordeaux, University of Bordeaux, Bordeaux, France; [15]Department of Pathology, Le Mans Hospital Center, Le Mans, France; [16]University Paris Est Créteil, INSERM, IMRB, Créteil, France; [17]Department of Immunobiology and INSERM U955, Henri Mondor University Hospital, Créteil, France; [18]Department of Hematology, University Hospital of Lille, Lille, France; [19]Department of Hematology, University Hospital of Rennes, Hospital Pontchaillou, Rennes, France; [20]Department of Oncology, Louis Pasteur Clinic, Essey-Lès-Nancy, France; [21]AP-HP, Henri Mondor Hospital, Lymphoid Malignancies Unit, Créteil, France; [22]Service of Hematology, Department of Oncology, Lausanne University, Hospital and Lausanne University, Lausanne, Switzerland; [23]Department of Hematology, Hospital of Lens, Lens and Department of Hematology, University Hospital of Amiens, Amiens, France; [24]Department of Hematology, Institute Curie, Hospital Rene Huguenin, Saint-Cloud, France; [25]Department of Hematology, Sud-Francilien Hospital Center, Corbeil-Essonnes, France; [26]Department of Hematology, Hospital Center of Blois, Blois, France; [27]Department of Hematology, Hospital Center Le Mans, Le Mans, France; [28]Department of Hematology, Center Hospitalier Lyon Sud and INSERM U1111, Pierre Bénite, France and [29]Institute of Human Genetics, Ulm University and Ulm University Medical Center, Ulm, Germany

LV and DC contributed equally as co-first authors.
#PG, OT and LdL contributed equally as co-senior authors.

Correspondence: L. de Leval
Laurence.deleval@chuv.ch

Received: April 12, 2022.
Accepted: June 9, 2022.
Prepublished: June 16, 2022.

https://doi.org/10.3324/haematol.2022.281226

Abstract

Monomorphic epitheliotropic intestinal T-cell lymphoma (MEITL) is a rare aggressive T-cell lymphoma most reported in Asia. We performed a comprehensive clinical, pathological and genomic study of 71 European MEITL patients (36 males, 35 females, median age 67 years). The majority presented with gastrointestinal involvement and had emergency surgery, and 40% had stage IV disease. The tumors were morphologically classified into two groups: typical (58%) and atypical (i.e., non-monomorphic or with necrosis, angiotropism or starry-sky pattern) (42%), sharing a homogeneous immunophenotypic profile (CD3+ [98%] CD4- [94%] CD5- [97%] CD7+ [97%] CD8+ [90%] CD56+ [86%] CD103+ [80%]

cytotoxic marker+ [98%]) with more frequent expression of TCRγδ (50%) than TCRαβ (32%). MYC expression (30% of cases) partly reflecting *MYC* gene locus alterations, correlated with non-monomorphic cytology. Almost all cases (97%) harbored deleterious mutation(s) and/or deletion of the *SETD2* gene and 90% had defective H3K36 trimethylation. Other frequently mutated genes were *STAT5B* (57%), *JAK3* (50%), *TP53* (35%), *JAK1* (12.5%), *BCOR* and *ATM* (11%). Both *TP53* mutations and MYC expression correlated with atypical morphology. The median overall survival (OS) of 63 patients (43/63 only received chemotherapy after initial surgery) was 7.8 months. Multivariate analysis found a strong negative impact on outcome of MYC expression, *TP53* mutation, *STAT5B* mutation and poor performance status while aberrant B-cell marker expression (20% of cases) correlated with better survival. In conclusion, MEITL is an aggressive disease with resistance to conventional therapy, predominantly characterized by driver gene alterations deregulating histone methylation and JAK/STAT signaling and encompasses genetic and morphologic variants associated with very high clinical risk.

Introduction

Monomorphic epitheliotropic intestinal T-cell lymphoma (MEITL), formerly considered as a variant (type II) of enteropathy-associated T-cell lymphoma (EATL), is now recognized a separate entity based on distinct clinicopathological and epidemiological features, unrelated to celiac disease (CD).[1] MEITL and EATL are both rare accounting together for less than 5% of peripheral T-cell lymphomas.[2,3] Many published series describe hybrid cohorts comprising MEITL and EATL.[4-8] In Western countries, the incidence of MEITL is even lower than the incidence of EATL. In contrast, in Asia where CD essentially does not exist, MEITL is the most common type of primary gastrointestinal T-cell lymphoma.[9-15]

As opposed to EATL, MEITL is defined as a tumor composed of monomorphic medium-sized cells, with round nuclei and a rim of pale cytoplasm, typically showing striking infiltration of intestinal epithelium and lacking necrosis or significant inflammation.[1,16] EATL and MEITL have in common an activated cytotoxic T-cell immunophenotype while distinctive MEITL features include expression of CD8 and CD56, negativity for CD30 and occasional CD20 expression.[4-6, 8,10-14,17,18]

The mutational landscape of MEITL encompasses frequent activating mutations of the JAK/STAT signaling pathway mainly affecting *STAT5B* (33-65%), *JAK3* (33-67%) and *JAK1* (5-44%).[7,18-23] Moreover, activating hotspot mutations in the *GNAI2* gene coding for guanine nucleotide-binding protein G(i), α-2 subunit have been reported in 21% of the cases in a study from Singapore.[20] We reported highly recurrent (>90%) deleterious alterations in the *SETD2* gene coding for SET Domain Containing 2, a histone lysine methyltransferase, which has been variably confirmed in subsequent studies.[7,18,20,23]

MEITL usually presents as a small bowel tumor often manifesting by perforation or obstruction, abdominal pain and weight loss. The disease follows an aggressive course with a median OS usually of less than 1 year (range, 6.5-14 months).[6,8,9,13,18,24] No robust prognostic or predictive biomarkers have been described to date.

Here, we studied a large series of 71 MEITL cases from Western Europe, performed histopathological assessment supplemented by extensive immunophenotyping, targeted fluorescence *in situ* hybridization (FISH) studies, and mutational analysis of a selected 27-gene panel in 65 cases. We present a comprehensive analysis integrating the pathological and molecular features and their correlation to clinical outcome.

Methods

Patients and samples

Seventy-one patients diagnosed with MEITL between 2005 and 2021 according to 2008 or 2017 World Health Organization classifications[1,16] (69 diagnostic and 2 relapse samples, all routinely processed formalin-fixed paraffin embedding [FFPE] tissues) were collected through the Tenomic Consortium of the Lymphoma Study Association (LYSA)[25] (n=65) and the University Hospital of Tübingen, Germany (n=6). Twenty-nine cases were included in a previous study.[7] The clinical history and imaging studies were collected from the patients' files by the treating physicians. The study was approved by the Commission antonale d'éthique de la recherche sur l'être humain (CER-VD, protocol 382/14), the Comité de Protection des Personnes-Ile-de-France IX (CPP08/009), and the Ethical Committee of the University of Tübingen (105/2013BO2) in accordance with the Declaration of Helsinki.

Histology, immunohistochemistry and fluorescence *in situ* hybridization

Diagnostic slides were reviewed. Additional immunostains and EBER *in situ* hybridization for detection of the Epstein-Barr virus (EBV) were performed using standard protocols (see the *Online Supplementary Appendix*; *Online Supplementary Table S1*). Immunostainings were evaluated semi-quantitatively by at least two pathologists. For most markers a five-tier scale was used (<5%, 5-25%, 26-50%, 51-75%, 76-100%), and a threshold of 5% was considered for positive score. Ki-67, MYC and p53 staining were

scored into quartiles (<25%, 26-50%, 51-75%, 76-100%). For FISH evaluation of the *SETD2* and *MYC* gene loci we used a homemade *SETD2* probe[7] and the commercial LSI *MYC* Dual Color Break Apart probe (8q24) (Abbott Molecular, Des Plaines, IL, USA) (*Online Supplementary Appendix*). Chromogenic slides were digitalized using a NanoZoomer S60 Digital slide scanner (Hamamatsu Photonics, Japan) at 40x magnification and evaluated using a digital image viewer system (TM-Microscopy, Telemis, Belgium). Morphology, IHC and FISH results were recorded in a coded dataset (*Online Supplementary Figure S1*).

Deep sequencing and mutation analysis

Sixty-five cases were examined by next-generation sequencing (NGS). Data were generated by whole-exome sequencing (WES) in 34 cases, including 14 previously reported,[7] and by targeted deep sequencing (TDS) using a customized 27-gene panel relevant to T-cell lymphoma biology in 29 cases, or a 9-gene panel TDS assay[7,26] in two cases. For WES, libraries from tumor and matched non-tumor DNA, both extracted from FFPE tissues, were paired-end sequenced on a HiSeq 4000 instrument (Illumina, San Diego, CA). For TDS, libraries of tumor DNA prepared with the KAPA HyperPlus kit (Roche, Pleasanton, CA) were target enriched by capture prior to sequencing on a MiSeq system (Illumina). After demultiplexing, alignment and duplicate removal, single nucleotide and indel variant calling was performed using three caller algorithms VarScan (v2.4.4) and MuTect2 algorithm (GATK v4.1). For WES set, the variant call was restricted to the 27 genes of the TDS panel plus *GNAI2*.

Statistical methods

Fisher's exact or χ^2 tests were used to determine associations between morphological, immunophenotypical and genetic characteristics. Estimates of overall survival were constructed using the Kaplan-Meier method. Cox proportional hazards regression model was used to investigate associated prognostic factors in univariate and multivariable analysis. In order to ensure the robustness of our results, the final model was validated by a two-step bootstrapping process. Results were expressed as hazard-ratio (HR) and 95% confidence interval (CI). Statistical analysis was performed using Stata software (version 15, StataCorp LP, College Station, US). The tests were two-sided, with a type I error set at 5%. When appropriate, a correction of the type I error was applied to take into account multiple comparisons.

Results

Patients' characteristics

The 36 male and 35 female patients had a median age of

Table 1. Clinical and biological features of monomorphic epitheliotropic intestinal T-cell lymphoma at diagnosis.

Features	MEITL patients (N=71)
Median age, years (range)	67 (29-91)
Male, N (%)	36 (51%)
Medical History*	
Prior coeliac disease	0/62 (0%)
Previous cancer	6/62 (10%)
Auto-immune disease	2/62 (3%)
Symptom history** median duration, months (range)	<1m (0-20)
Abdominal pain	48/54 (89%)
Weight loss	34/54 (63%)
Fatigue	36/54 (67%)
Anorexia	28/54 (52%)
Diarrhea	15/54 (28%)
Palpable abdominal mass or adenopathy	10/54 (18%)
Acute event at presentation***	52/61 (85%)
Bowel perforation	43/61 (70%)
Bowel obstruction	17/61 (28%)
Performance Status	
0-1	27/56 (48%)
2	15/56 (27%)
>2	14/56 (25%)
Lugano stage	
Stage I	20/60 (33%)
Stage II	16/60 (27%)
II.1	9/60 (15%)
II.2	1/60 (2%)
IIE	3/60 (5%)
Not specified	3/60 (5%)
Stage IV	24/60 (40%)
Elevated serum LDH	18/32 (56%)
Hypoalbuminemia (<35 g/L)	27/33 (82%)
Surgical management	59/63 (94%)
No chemotherapy	19/62 (31%)
First-line regimens	43/62 (69%)
CHOP-based (CHOP, CHOEP, Ro-CHOP, R-CHOP)	32/43 (74%)
CHOP + IVE-MTX	6/43 (14%)
Other treatments (COP, ACVBP, DDGP, radiotherapy)	4/43 (9%)
Unknown	1/43 (2%)
First-line consolidation****	9/43 (21%)
Response (at end of first line)	
Complete response	15/43 (35%)
Partial response	4/43 (9%)
Stable disease	2/43 (5%)
Primary progression	20/43 (46%)
Death with unknown status	1/43 (2%)
Unknown	1/43 (2%)
Progression/relapse after first-line	36/42 (86%)
Salvage treatment after progression/relapse	30/36 (83%)
Salvage treatment consolidation	3/30 (10%)
Number of lines of treated patients: median, N (range)	1 (1-5)

MEITL: monomorphic epitheliotropic intestinal T-cell lymphoma; LDH: lactate dehydrogenase; PS: performance status; CHOP: cyclophosphamide, doxorubicin, vincristine, prednisone; CHOEP: cyclophosphamide, doxorubicin, vincristine, etoposide, prednisone; Ro-: Romidepsin; R-: Rituximab; IVE-MTX: ifosfamide, epirubicin, etoposide, methotrexate; COP: cyclophosphamide, vincristine, prednisone; ACVBP: doxorubicin, cyclophosphamide, vindesine, bleomycin, prednisone; DDGP: cisplatin, dexamethasone, gemcitabine, and pegasparaginase ; auto-HCT: autologous hematopoietic cell transplantation; allo-HCT: allogeneic hematopoietic cell transplantation ; OS: overall survival. *Cancer cases: colorectal cancer (n=1), cutaneous T-cell lymphoma (n=1), essential thrombocytemia (n=1), prostatic cancer (n=1), breast cancer (n=2). Autoimmune disease: autoimmune thyroiditis (n=1), giant cell arteritis (n=1). **Other symptoms not reported in the table included night sweats (n=5), pruritus (n=2), bleeding, pancreatitis, pleural effusion, pulmonary embolism, abdominal abscess, intestinal ulcers (n=1 for each). ***Patients with perforation occurring after the start of chemotherapy are not included. **** Including autoHCT (n=8) and alloHCT (n=1).

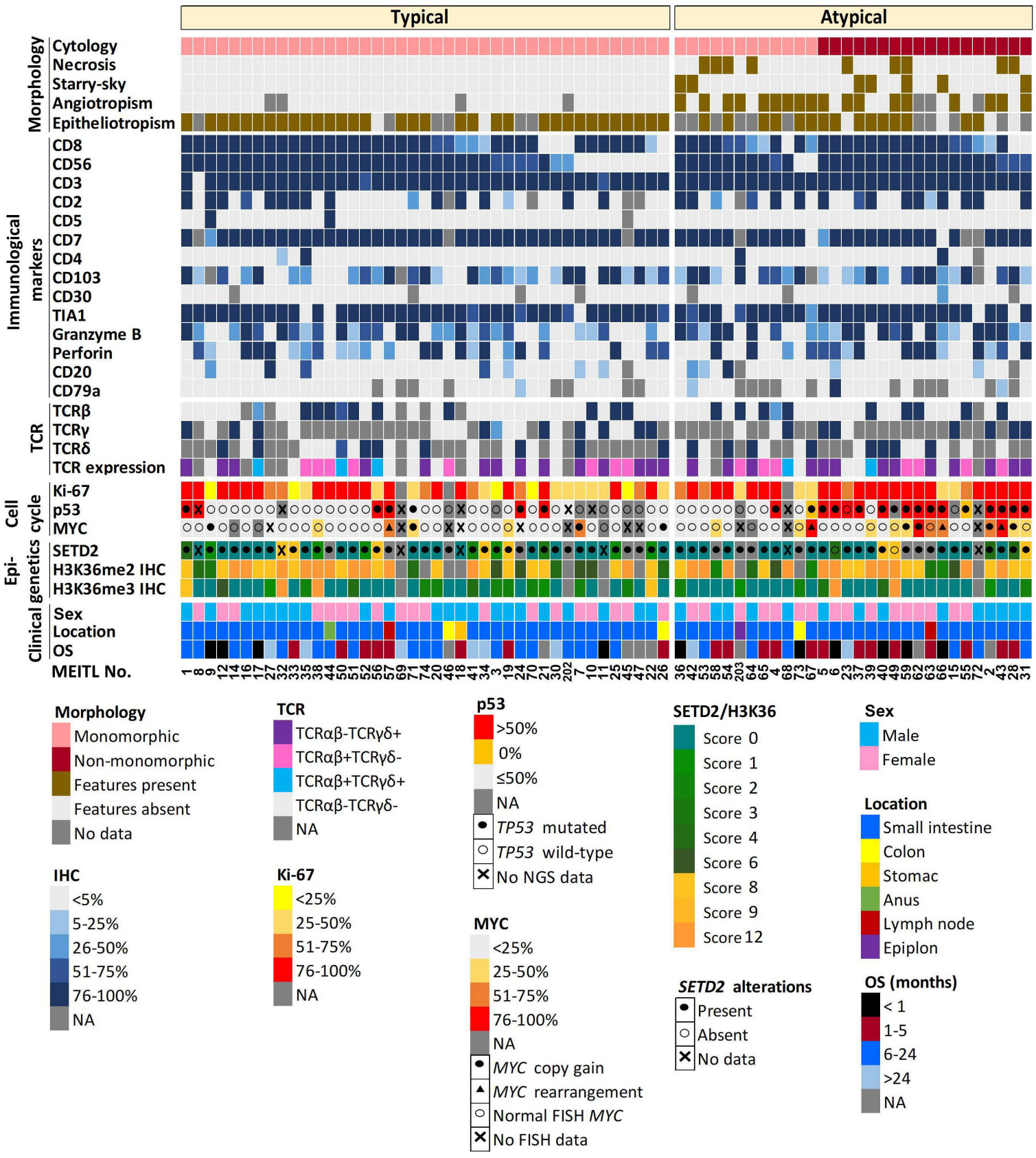

Figure 1. Heatmap representation of morphological, immunophenotypical and molecular features of 71 monomorphic epitheliotropic intestinal T-cell lymphoma patients. TCR: T-cell receptor; IHC: immunohistochemistry; FISH: fluorescence *in situ* hybridization; OS: overall survival; NA: not available; NGS: next-generation sequencing.

67 years (range, 29-91 years). Baseline clinical and biological features of 63 patients are presented in Table 1 and *Online Supplementary Tables S2 and S3*. All had gastrointestinal involvement, most often restricted to the small intestine (n=46/63, 73%) and most patients (52/61, 85%) presented with acute symptoms, mainly related to intestinal perforation and/or obstruction. According to the Lugano staging system: 33% (n=20) had only GI involvement (stage I), 27% (n=16) had local or abdominal lymph nodes (stage II), 40% (n=24) were stage IV with supradiaphragmatic lymph nodes or extradigestive/extranodal involvement, most commonly pleuro-pulmonary (n=7), or hepatic (n=4).

Histopathology

The main histopathological features are summarized in Figure 1. The size of intestinal tumors ranged from 1.7 to 20 cm (median 6 cm). Except for one case with mainly mucosal involvement, 61 of 62 (98%) surgical specimens comprised a frequently ulcerated transmural central zone, perforated in 44 of 58 cases (76%), and showed lateral tumor extension predominant in the mucosa (peripheral zone)[10,17] in 40 of 46 (87%) evaluable cases (Figure 2A).

Most intestinal cases (48/54, 89%) showed tumor epitheliotropism (Figure 1; Figure 2B, D and E). Morphology of other tumor locations with epitheliotropism in non-intestinal sites are illustrated in the *Online Supplementary Figure S2A* to *H* and Figure 3J to L.

Most cases (53/71, 75%) showed classical monomorphic cytology, i.e., round and small/medium-sized tumor cells with little variation in nuclear size, slightly dispersed chromatin, inconspicuous nucleoli, and ample pale cytoplasm (Figure 2B and C). However, a significant proportion of

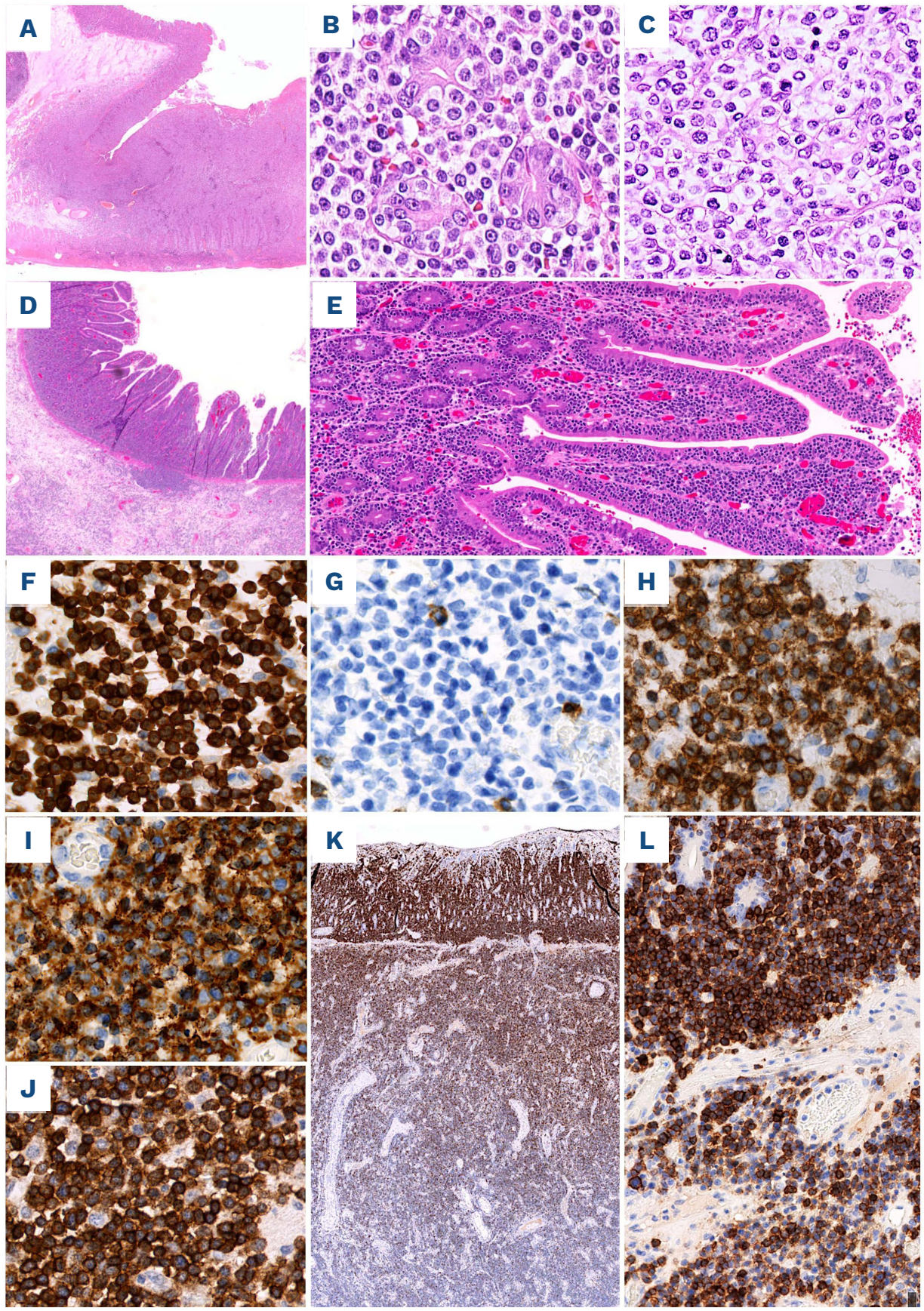

Figure 2. Typical monomorphic epitheliotropic intestinal T-cell lymphoma cases #30 (A to C) and #51 (D to L). (A) The intestinal tumor comprises a central transmural zone and a peripheral zone with intramucosal tumor spread. (B) The tumor cells are medium-sized and monomorphic with clear and ample cytoplasm and invade the epithelium of the crypts. (C) The tumor recurrence after 5 years shows an identical cytomorphology. (D) Intramucosal tumor spread is associated with shortening and widening of the villi. (E) Broadly expanded villi comprise a heavy epitheliotropic tumor cell infiltrate. (F) The tumor cells are strongly positive for CD3, (G) negative for CD5, (H) positive for CD8, (I) CD56, and (J) TCRβ. (K) CD103 is strongly positive in the superficial intramucosal tumor compartment and gradually decreases in the infiltrating part. (L) Lymphoma cells in the mucosa (upper part of panel figure) and submucosa (lower part of panel figure) are strongly and moderately positive for CD103. Original magnifications x10 (A), x40 (K), x100 (E), x125 (D), x400 (B, C, F to J, L).

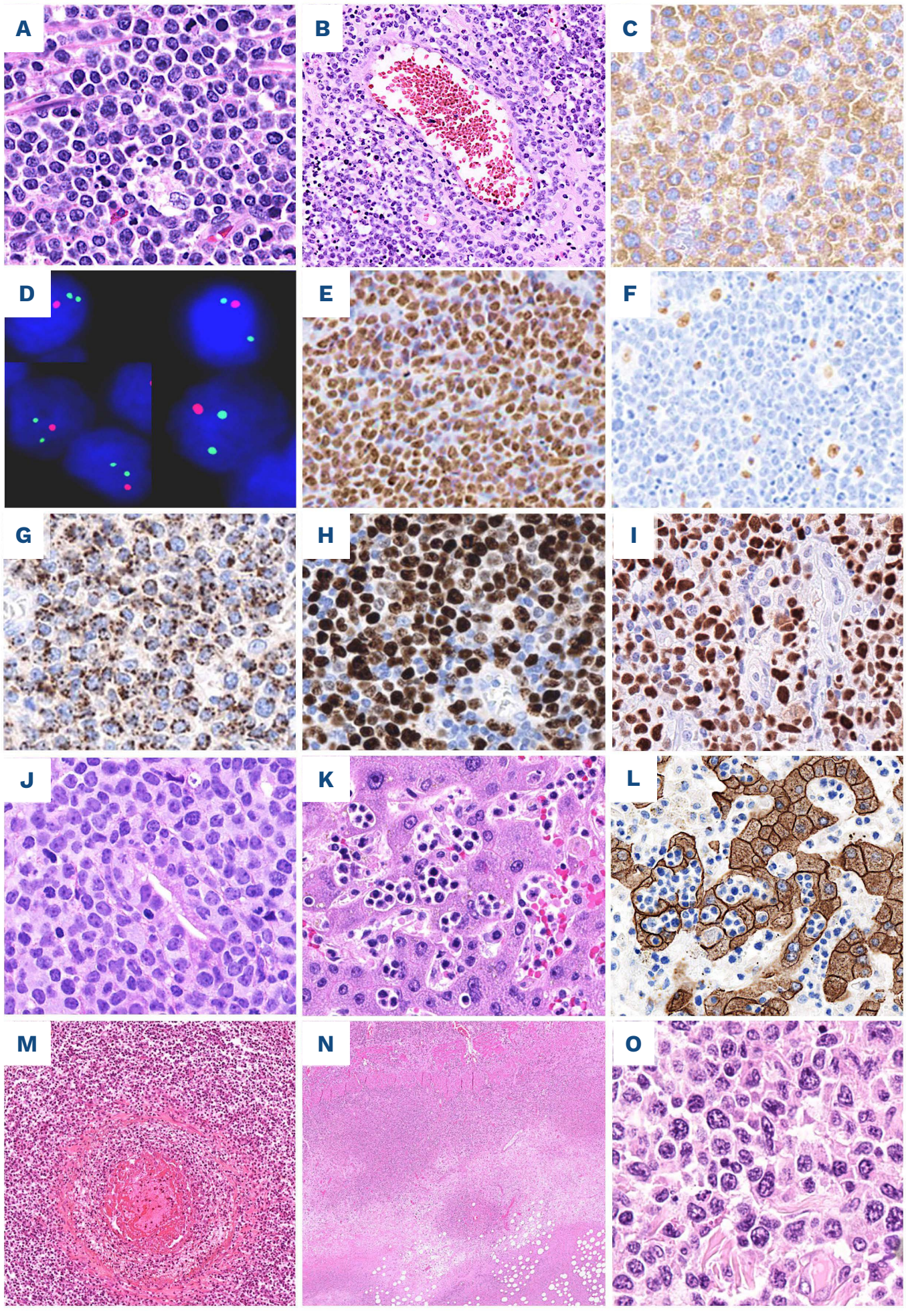

Figure 3. Atypical monomorphic epitheliotropic intestinal T-cell lymphoma cases #31 (A to L), #15 (M) and #59 (N to O). (A) The tumor is composed of medium–sized pleomorphic cells and comprises scattered histiocytes with apoptotic debris. (B) A vein is infiltrated by lymphoma cells. (C) The lymphoma cells are weakly positive for TCRγ. (D) FISH with *SETD2* probe shows 1 red (*SETD2*) and 2 green (control) signals per nucleus, indicating deletion of 1 allele. (E) The lymphoma cells show strong nuclear positivity for H3K36me2 and (F) are completely negative for H3K36me3, while reactive histiocytes are positive. (G) The lymphoma cells are diffusely positive for TIA-1, (H) show a high Ki67 index (>80%), and (I) are strongly positive for p53. (J) A gastric biopsy performed during follow-up showed recurrent tumor with a more blastoid morphology, invading the glandular epithelium. (K) Post-mortem liver showed lymphoma infiltrating in the sinusoids and within hepatocytes. (L) A cytokeratin immunostains confirmed emperipolesis of lymphoma cells into hepatocytes. (M) This case features marked angiotropism and angioinvasion. (N) This tumor contains large necrotic areas in its invasive portion, and (O) is composed of pleomorphic large cells. Original magnifications: x25 (N), x100 (B and M), ×400 (A, C, E to K, L, O), x630 (D).

cases (18/71, 25%) showed either significant cellular pleomorphism, larger cell size, vesicular chromatin and/or prominent nucleoli (Figure 3A and O; *Online Supplementary Figure S3D* to *F*). A peculiar, atypical case (#66) had two distinct monomorphic and non-monomorphic components (*Online Supplementary Figure S4*). Except for two non-monomorphic cases, which had abundant eosinophils and prominent plasma cells, all cases presented very few inflammatory cells. Mitoses were easily identified in most cases. While mitoses were easily identified in most cases, a small subset (7/71 cases, 10%), appeared as high-grade neoplasms with a "starry-sky" pattern or abundant apoptotic debris (Figure 3; *Online Supplementary Figure S3A* to *C*). Other unusual features were seen in a subset of cases: coagulative necrosis distinct from surface ulceration in 9 cases (Figure 3N), or focal or prominent angiotropism or angioinvasion of medium to large-sized blood vessels in 18 cases (Figure 3B and M), which were frequent among non-monomorphic cases (*Online Supplementary Table S4*). Overall, we distinguished two morphological groups of cases: typical tumors (n=41, 58%) and atypical tumors (n=30, 42%) featuring one or more atypical histological characteristic(s) (Figure 1; Table 2).

Immunophenotype and Epstein-Barr virus status

The immunophenotypic profiles are shown in Figure 1 and summarized in Table 2. Most cases had homogeneous and strong expression of CD3 (70/71, 99%) and CD7 (63/65, 97%). CD2 was positive in 32 of 66 cases (48%). Only two of 70 (3%) cases were CD5-positive. CD8 and CD56 were usually widely expressed, but with heterogeneous staining intensity. Most cases (55/71, 77%) were positive for both CD56 and CD8, nine of 71 (13%) were CD8+ CD56-, six of 71 (8%) were CD8- CD56+, and one case CD8- CD56-. Four cases, all CD8+ CD56+, were strongly CD4-positive. CD30 was negative in all cases (63/64, 98%), except in occasional large, atypical cells in case #66 (*Online Supplementary Figure S4*). PD1 was negative in 20 of 20 tested cases. Most cases strongly expressed TIA1 in most tumor cells (65/68, 96%) (Figure 3G); but immunostains for granzyme B and perforin, positive in 50 of 66 cases (76%) and 39 of 62 cases (63%) respectively, were frequently weaker with often <50% positive tumor cells. Overall, 59 of 68 (87%) cases had an activated cytotoxic profile, 11 cases expressed TIA1 only and one case was negative for the three cytotoxic markers.

Half of cases (32/64, 50%) expressed TCRγ and/or TCRδ (TCRγδ+), and 21 of 65 (32%) cases were positive for TCRβ (TCRαβ+). Sixty-two cases with contributory results for both TCR isoforms were classified as single positive for TCRγδ (43%) (Figure 3C) or TCRαβ (24%) (Figure 2J), TCR silent (24%), or double positive (9%) (*Online Supplementary Figure S3G* to *I*).

Fifty-two of 65 cases (80%) were CD103-positive. Apart from few cases homogeneously and intensely CD103-positive, in most cases a gradient of staining was observed from more intense and extensive in the intramucosal portion to weaker or negative in the deeper infiltrative part (Figure 2K to L).

Co-expression of CD20, usually by <50% of the tumor cells and weaker than in normal B cells, was observed in 12 of 67 (18%) cases. Four of 51 (8%) cases were CD79a+. Two cases co-expressed CD20 and CD79a (*Online Supplementary Figure S3A* to *C*), but lacked PAX5 and were positive for CD8, CD56 and cytotoxic markers. All 24 tested cases for PAX5 were negative. In total, 14 of 67 (20%) were B-cell marker-positive.

Ki-67 proliferation index was >75% in most cases (38/68, 56%) (Figures 1 and 3H). All 68 cases tested for EBV by EBER-ISH were negative, and one case showed scattered reactive small (<1%) EBV-positive cells.

There were no significant differences in the immunophenotypic profiles of atypical and typical cases (Table 2; *Online Supplementary Table S4*).

SETD2 gene alterations and defective H3K36me3 trimethylation

By NGS analysis (*Online Supplementary Table S5*; Figure 4A), we found a very high prevalence of *SETD2* mutations in 59 of 65 cases (91%), with two mutations in 29 of 59 cases (49%) and three mutations in one case (#59) (Figure 4B). Of the 88 *SETD2* mutations identified, 62 (27 nonsense, 26 frameshift and 9 splice-sites) were likely generating a truncated non-functional protein and were distributed throughout the whole gene domains. Moreover, most of the 24 missense mutations clustered within the SET domain of the *SETD2* protein or its proximity. Notably, the 24 cases analysed by both WES and TDS (this latter only on the tumor component) showed complete overlap, indicating absence of germline variants in this subset of patients. Heterozygous deletions of *SETD2* were observed in nine of 57 (16%) cases evaluated by FISH, of which six had one or two concurrent *SETD2* mutation(s), and three were *SETD2* wild-type (Figure 3D). Overall, of 54 cases with complete NGS and FISH results for *SETD2*, 23 had one mutation or deletion, 29 had two or more alterations and only two had no detectable alteration. These latter two cases (#6 and #49) were non-monomorphic, with a characteristic CD8+, CD56+, TCRγδ+ cytotoxic phenotype, and harbored other mutations in the JAK/STAT pathway.

Immunohistochemistry was performed to assess the SETD2–H3K36me2–H3K36me3 axis at the protein level (Figure 1). Defective expression of SETD2 or H3K36me3 (IHC scores ≤6) were observed in 47 of 55 cases (85%) and 60 of 66 cases (91%), respectively. The correlation between *SETD2* gene alterations and SETD2 protein expression (Figure 1) was concordant in 43 of 50 cases

(86%); six cases with *SETD2* gene alteration had preserved SETD2 expression, and one case had defective protein expression and no detectable gene alteration. H3K36me3 IHC results were concordant with the *SETD2* status, in 60 of 63 cases (95%) i.e., 58 cases had defective H3K36me3 trimethylation (H3K36me3 score ≤6) and altered *SETD2*, and two cases with high H3K36me3 scores had no detected *SETD2* alteration. Only three cases, two with monoallelic alteration and one with double mutations of *SEDT2*, had high H3K36me3 scores. Thus, H3K36me3 IHC as a surrogate to identifying *SETD2* gene alterations was highly sensitive (95%), and 100% specific (K=0.55, 95% CI:

Table 2. Morphological, immunophenotypical and molecular characteristics of typical and atypical groups.

	All cases (N=71)	Typical (N=41)	Atypical (N=30)	Adjusted *P*
Morphology				
Non-monomophic	18/71 (25.3%)	0/41 (0%)	18/30 (60%)	**<0.0001** *
Necrosis	9/71 (12.6%)	0/41 (0%)	9/30 (30%)	**<0.0001** *
Starry-sky/apoptosis	7/71(9.8%)	0/41 (0%)	7/30 (23.3%)	**0.002** *
Angiotropism	18/64 (28.1%)	0/37 (0%)	18/27 (66.6%)	**<0.0001** *
Lack of epitheliotropism	6/54 (11.1%)	2/35 (5.7%)	4/19 (21.0%)	0.169
Immunological markers				
CD8	64/71 (90.1%)	37/41 (90.2%)	27/30 (90%)	1.000
CD56	61/71(85.9%)	33/41 (80.4%)	28/30 (93.3%)	0.174
CD3	70/71(98.5%)	40/41 (97.5%)	30/30 (100%)	1.000
CD2	32/66 (48.4%)	16/37 (43.2%)	16/29 (55.1%)	0.457
CD5	2/70 (2.8%)	2/40 (5%)	0/30 (0%)	0.503
CD7	63/65 (96.9%)	38/38 (100%)	25/27 (92.5%)	0.169
CD4	4/70 (5.7%)	2/41 (4.8%)	2/29 (6.8%)	1.000
CD103	52/65 (80%)	29/38 (76.3%)	23/27 (85.1%)	0.532
CD30	1/64 (1.5%)	0/37 (0%)	1/27 (3.7%)	0.422
TIA1	65/68 (95.5%)	38/41 (92.6%)	27/27 (100%)	0.271
Granzyme B	50/66 (75.7%)	27/38 (71.0%)	23/28 (82.1%)	0.388
Perforin	39/62 (62.9%)	23/36 (63.8%)	16/26 (61.5%)	1.000
CD20	12/67 (17.9%)	7/40 (17.5%)	5/27 (18.5%)	1.000
CD79a	4/51 (7.8%)	1/32(3.1%)	3/19 (15.7%)	0.140
Epigenetics				
SETD2 (score >8)	8/55 (14.5%)	5/33 (15.1%)	3/22 (13.6%)	1.00
H3K36me3 (score >8)	6/67 (8.9%)	4/38 (10.5%)	2/29 (6.8%)	0.69
TCR expression				
TCRβ	21/65 (32.3%)	11/36 (30.5%)	10/29 (34.4%)	0.794
TCRγ/δ	32/64 (50%)	17/36 (47.2%)	15/28 (53.5%)	0.801
TCRαβ-TCRγδ+	27/62 (43.5%)	14/34 (41.1%)	13/28 (46.4%)	0.955
TCRαβ+TCRγδ-	15/62 (24.1%)	8/34 (23.5%)	7/15 (46.6%)	
TCRαβ+TCRγδ+	5/62 (8.0%)	3/34 (8.8%)	2/28 (7.1%)	
TCRαβ-TCRγδ-	15/62 (24.1%)	9/34 (26.4%)	15/62 (24.1%)	
Cell cycle				
Ki-67 >50%	48/68 (70.5%)	24/39 (61.5%)	24/29 (82.7%)	0.066
MYC >25%	18/54 (33.3%)	5/30 (16.6%)	13/24 (54.1%)	**0.008**
p53 IHC mutated pattern	22/56 (39.2%)	6/31 (19.3%)	16/25 (64%)	**0.001**
Genetics				
TP53 mutation	22/64 (34.3%)	6/36 (16.6%)	16/28 (57.1%)	**0.001**
MYC alteration	12/60 (20%)	5/33 (15.1%)	7/27 (25.9%)	0.345
SETD2 alteration	62/64 (96.8%)	36/36 (100%)	26/28 (92.8%)	0.188
STAT5B mutation	37/65 (56.9%)	20/37 (54.0%)	17/28 (60.7%)	0.622
JAK3 mutation	32/64 (50%)	19/36 (52.7%)	13/28 (46.4%)	0.801

* Expected correlation (by definition). ICH: immunohistochemistry; TCR: T-cell receptor.

0.11-0.99; *P*<0.015) (Figure 3E to F; *Online Supplementary Figure S5*)

Mutations in other genes

The second most frequently mutated gene was *STAT5B* featuring alterations in 37 of 65 cases (57%) (Figure 4). *STAT5B* mutations were all missense, single (n=31) or double (n=6). Most mutations (70%) occurred in the SH2 domain, including the hotspot N642H activating mutation in 21 patients.[7] *JAK3* mutations found in 32 of 64 cases

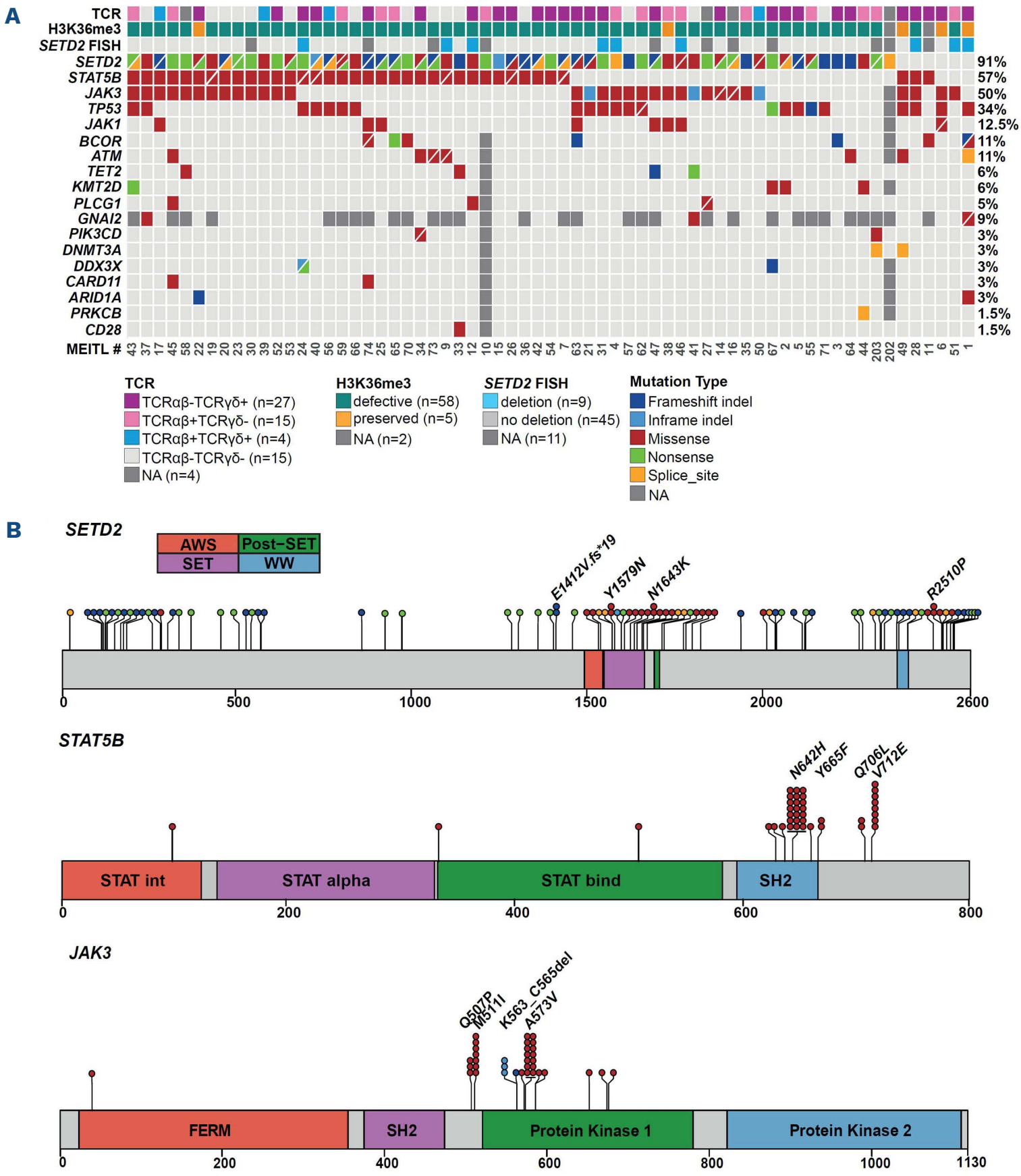

Figure 4. Overview of the genetic alterations in monomorphic epitheliotropic intestinal T-cell lymphoma. (A) Heatmap representation of mutations in a selected panel of genes examined by whole-exome sequencing and targeted deep sequencing in 65 monomorphic epitheliotropic intestinal T-cell lymphoma (MEITL) tumors. Patients are displayed as columns and mutations (named on the left) are coloured by the type of alteration. The percentage of mutated samples is represented on the right. First row shows the expression patterns of T-cell receptor (TCR) isoforms, second row shows the status of H3K36me3 trimethylation and third row displays the results of *SETD2* fluorescence *in situ* hybridization (FISH) study. (B) Schematic representation of somatic mutations in *SETD2* (top), *STAT5B* (central) and *JAK3* (bottom) genes identified in this study. Domains of the protein are represented according to the Uniprot database (http://www.uniprot.org) in different colors. Exact positions of mutations found in MEITL cases are given, which are colored by the type of alteration.

(50%) included several activating variants clustered in the pseudokinase domain (such as A573V, M511I, R657W, K563_566del, P676R), and were single (n=29) or double (n=2). *JAK1* mutations were identified in a smaller proportion of cases (8/64, 12%). Mutations in *STAT5B*, *JAK3* and *JAK1* were not mutually exclusive. In all, 54 of 64 cases (84%) had mutations in at least one gene of the JAK/STAT pathway. Notably, *STAT5B* mutations showed significantly higher allele frequencies than *JAK3* and *SETD2* mutations, likely due to co-occurring loss-of-heterozygosity (LOH) or allelic imbalance events (*Online Supplementary Figure S6*). *TP53* mutations were identified in 22 of 63 (35%) cases and, similar to *STAT5B* mutations, were also associated with a high-allele frequencies due to copy number losses or copy number neutral LOH events (*Online Supplementary Figure S6*). Remarkably, *TP53* mutations occurred mostly among the atypical group (adjusted *P*=0.01, Fisher's exact test) (Table 2) and correlated with abnormal p53 IHC pattern – either overexpression (>50%) or uncommonly completely negative staining in 2 cases (adjusted *P*<0.001, Fisher's exact test) (Figures 1 and 3I; *Online Supplementary Table S4*).

Mutations in *BCOR* and *ATM* were found in 11% of cases each. Three of 34 cases (9%) carried somatic mutations in the *GNAI2* gene; two in codon R179 previously described,[20] and one p.T182I mutation.

MYC status

Twelve of 60 cases subjected to FISH (20%) had *MYC* gene locus alterations, i.e., copy gains in eight and breaks (rearrangements) in four cases. None of the cases with *MYC* copy gain was hyperploid (*Online Supplementary Appendix*). Ten of the 12 cases with *MYC* gene alterations had >25% MYC protein-positive tumor cells by immunohistochemistry. Overall, MYC expression was detected in 18 of 54 cases (33%), more frequently among non-monomorphic tumors (adjusted *P*=0.008, Table 2). Altered MYC status (by FISH or IHC) also tended to correlate with *TP53* mutations (adjusted *P*=0.05 and 0.06, respectively), and nine cases harboured both *TP53* mutations and *MYC* gene rearrangement (n=4) or copy gains (n=5) (Figure 1; *Online Supplementary Figure S3D* and *F*; *Online Supplementary Table S4*).

Treatment and outcome

Treatments and outcomes of 63 patients are summarized in Table 1. Most patients (59/63, 93%) underwent surgery and tumor resection. Seventeen patients with no further treatment died within a median time of 1 month. Of 43 patients who received a first-line therapy, one died before assessment and 20 progressed on treatment. Nine of 28 patients aged ≤65 years received consolidation with hematopoietic cell transplantation either autologous (auto-HCT) (n=8) or allogeneic (allo-HCT) (n=1). The 36 patients who relapsed following first-line therapy, often received one (or less commonly more) salvage treatment (30/36) and all died, usually from disease progression (n=31).

After a median follow-up of 46 months (alive patients), median overall survival (OS) was 7.8 months (range, 0-71). One-year and 2-year OS were 31% and 15%, respectively. In univariate analysis of OS (Figure 5; *Online Supplementary Table S6*): age>70, enterostomy, poor performance status (PS) (>2), advanced Lugano stage (≥2), lack of complete response to first-line therapy, atypical histology, MYC expression, and *TP53* mutations were all significantly associated with inferior outcome. Conversely, B-cell marker expression was associated with a better prognosis. The multivariate analysis confirmed the independent impact of *TP53* mutations (*P*=0.005, hazard ratio [HR] =5.83), *STAT5B* mutations (*P*=0.007, HR=3.67), B-cell (CD20 and/or CD79a) marker expression (*P*=0.005, HR=0.15) and poor PS (*P*=<0.001, HR=7.58) on OS (Table 3; *Online Supplementary Table S7*).

Eight patients survived beyond 24 months (*Online Supplementary Table S8*). They all had a good PS at diagnosis and underwent surgery. The seven patients who received chemotherapy (CHOP-based in 5) reached complete (6) or partial (1) response. Six cases were classified as typical and two as atypical, all lacked *TP53* mutations, and MYC expression, and four of eight were CD20+. In a very long survivor patient (#31) who relapsed 5 years after initial diagnosis, the relapsing tumor was also analyzed and showed a morphology and mutation profile identical to the initial diagnosis, and a very similar phenotype apart from reduced CD56 expression at relapse.

Discussion

This integrative clinical, histopathological and genetic analysis of 71 MEITL patients from Western Europe represents the largest study to date.

Our findings confirm that MEITL shows a rather homogeneous CD3+, CD4-, CD5-, CD7+, CD8+, CD56+ activated cytotoxic immunophenotype.[4,5,10-14,17,18] Most cases were CD8+ CD56+ and those negative for CD8 and/or CD56 (23%) did not show peculiar features. The distribution of TCR expression profiles is in line with the preferential γδ T-cell derivation reported in several studies.[4,5,11,17] In addition, TCRγδ+ and TCRαβ+ tumors showed similar pathological and mutational features, with no impact on outcome. Expression of CD103 (the α E subunit of the heterodimer integrin αEβ7), which is characteristic of intraepithelial lymphocytes of the small intestine and documented in T-cell lymphomas, particularly EATL,[27] was positive in most cases, albeit with heterogeneous staining. CD103 expression could therefore represent an additional

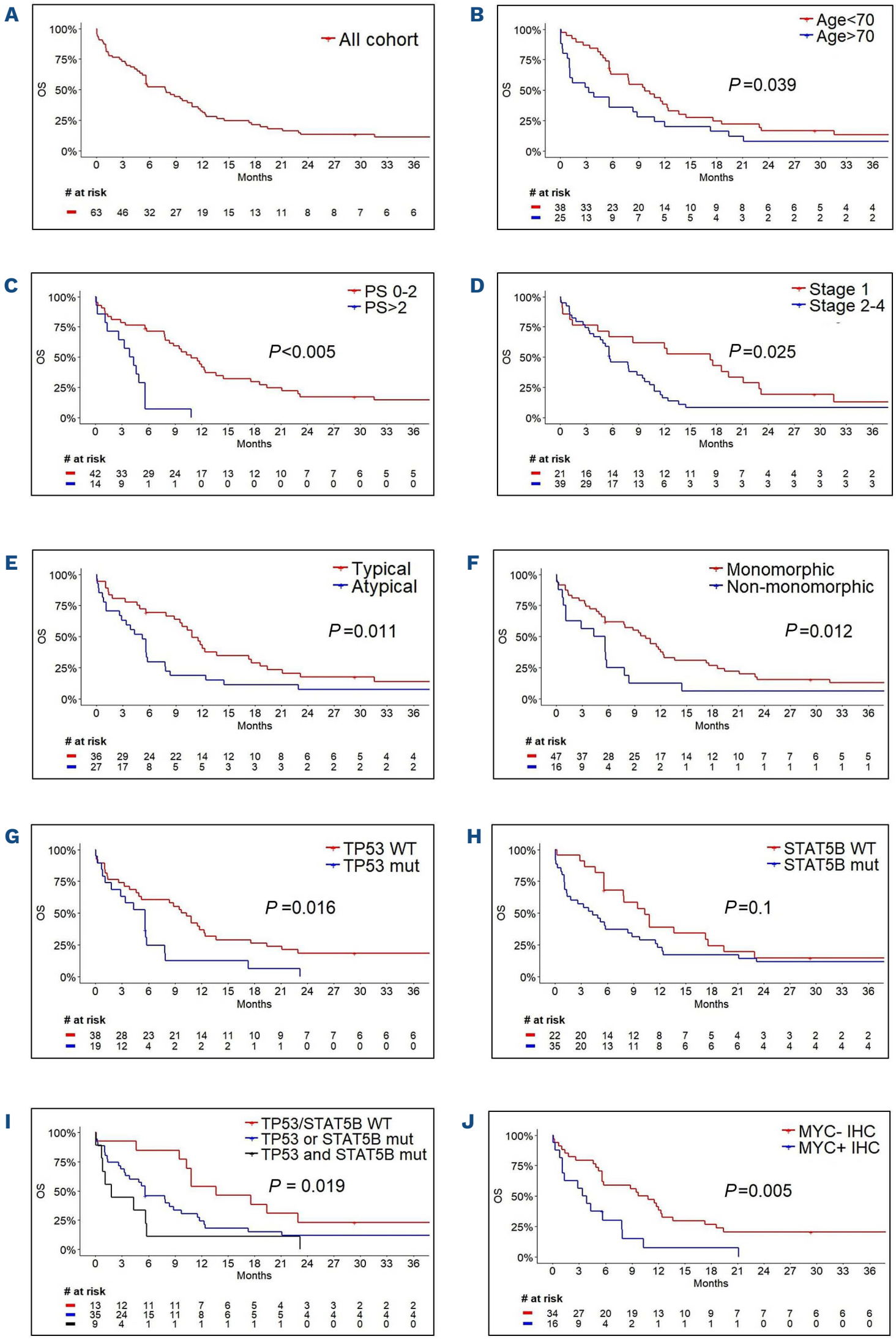

Figure 5. Overall survival for monomorphic epitheliotropic intestinal T-cell lymphoma patients. (A) Overall survival (OS) in months of the all cohort; and according to (B) age at diagnosis, (C) performance status (PS) score, (D) Lugano stage at diagnosis, (E) the presence of atypical histological features, (F) cytological atypia, (G) *TP53* mutational status, (H) *STAT5B* mutational status, (I) the concurrent presence of *TP53* and *STAT5B* mutations and (J) MYC expression (>25% immunohistochemistry). Age in years. MEITL: monomorphic epitheliotropic intestinal T-cell lymphoma; # at risk: number at risk; mut: mutated; WT: wild-type.

diagnostic feature of MEITL.

The mutational analyses reflect a very characteristic pattern of alterations involving frequent somatic deleterious alterations of *SETD2* (96%) and activation of JAK/STAT pathway gene(s), confirming our original discovery.[7] Moreover, *TP53* mutations and MYC deregulation occurred in a subset of cases. Intriguingly, while we also found 100% *SETD2* alterations in nine of nine cases from Japan,[23] a lower incidence of *SETD2* mutations was reported in other series, being ~70% in 23 Northern American cases[6] and 22% in 20 Chinese cases.[18] Along with the notion of many tumor suppressor genes requiring biallelic inactivation,[28] most cases had two *SETD2* alterations, with no evidences of germline variants. Notably, cases with apparently only one genetic hit had similarly reduced H3K36me3 histone mark, alluding to other mechanisms at play. Since functional studies have established the role of *SETD2* ablation in driving experimental lymphomagenesis,[29] our data support the key role of *SETD2* inactivation in MEITL pathogenesis. Conversely, mutations in other genes involved in DNA (and histone) methylation, in particular *TET2* and *DNMT3A*, were distinctly rare or absent contrasting with other T-cell lymphoma entities.[30,31] Thus, deregulated methylation of the H3K36 position represents the major epigenetic alteration in MEITL. For diagnostic purposes, NGS approaches interrogating the complete sequence of *SETD2* gene are mandatory since mutations are distributed without hot spots. In addition, we recommend analyses for the detection of *SETD2* locus loss or LOH. We showed that H3K36me3 IHC is an acceptable surrogate or complement to genotyping.

We identified two groups of tumors with distinct morphological features: a typical group of monomorphic tumors (58%) and an atypical group of tumors (42%), non-monomorphic, or presenting features suggesting a more aggressive biology. Some nuclear pleomorphism and large cell morphology have been recognized in Asian series but no association to clinical features or divergent immunophenotypes has been reported.[10,11,13,14,16,17] Here, while both groups shared similar immunophenotype and heterogeneous T-cell lineage derivation, the atypical group had more frequent MYC expression, *TP53* alterations, and a shorter overall survival in univariate analysis. Thus, our novel findings confirm and expand the notion that MEITL comprises a morphological spectrum, irrespective of ethnicity, including an atypical subgroup with meaningful biological attributes, and clinical relevance. The recognition that MEITL may show pleomorphism, angiotropism, necrosis, high-grade features or inflammation, is important for pathologists and relevant to diagnosis. It implies to consider atypical MEITL in the differential diagnosis of aggressive pleomorphic intestinal T-cell tumors, including EATL, EBV-associated extranodal NK/T-cell lymphoma, and intestinal T-cell lymphoma, NOS, which can be performed by the integration of clinical, immunophenotypic, H3K36me trimethylation status and mutational profile.

Median OS was only 7.8 months, on the lower end of the 7-15 months previously reported[9,10,18,24,32] perhaps related to the older age of our population and to a late diagnosis by an abdominal complication in most patients. Among baseline clinical parameters, univariate analysis found that age >70 years, PS >2 and Lugano stage ≥2 were associated with a worse prognosis. However, in multivariate analysis only PS >2 remained significantly associated with poor OS underlying the importance of patients' fitness to survive initial disease presentation and treatment. In addition, our study revealed biomarkers of independent unfavorable prognostic significance including *TP53* and *STAT5B* mutations and MYC expression. *TP53* alterations are well-known determinants of chemoresistance and worse outcome in lymphoma patients in general, and specifically in T-cell lymphomas.[33-36] Activating mutations of *STAT5B* mutations have an established role in T-cell lymphomagenesis;[37] they are frequent in several types of – usually aggressive - lymphomas derived from γδ or NK cells, and in a subset of T-large granular lymphocytic leukemias (T-LGL)[21,22,29,38,39] associated with a more aggressive behavior.[38] Accordingly, we found a striking negative effect of concurrent *TP53* and *STAT5B* mutations on survival.

In MEITL, gains of 8q24 or *MYC* copy gains have been variably reported in 25-70% of cases,[5,10,11,40] rare cases harboring *MYC* rearrangements have been described,[10,19] and

Table 3. Multivariate model of overall survival.

N of patients=44	HR	95% CI	*P* value
B-cell marker expression (IHC)	0.15	0.05-0.46	0.001
TP53 mutation	4.86	1.75-13.5	0.002
STAT5B mutation	3.42	1.44-8.13	0.005
MYC expression > 25% (IHC)	3.06	1.33-7.04	0.009
Performance Status ≥2	6.46	2.44-17.1	<0.001

IHC: immunohistochemistry; CI: confidence interval; HR: hazard ratio. For multivariable analysis, the covariates were determined according to univariate results ($P \leq 0.10$) and to the clinical and biological relevance, restricted to 44 cases with available pretherapeutic features (*Online Supplementary Table S7*; *Online Supplementary Statistical Methods*).

around half of cases reportedly show MYC protein expression.[5,15,19] We found MYC expression in one third of the cases, more frequently in atypical cases and in association with *TP53* mutations. Nine cases had concurrent *MYC* and *TP53* gene alterations, with six of seven patients dying within 5 months after diagnosis. The poor prognosis of patients with *MYC* plus *TP53* abnormalities has been reported in diffuse large B-cell lymphoma[41] along with high-grade morphology and also in chronic lymphocytic leukemia.[42] Thus, *MYC* and *TP53* aberrations may play a role in MEITL pathogenesis and progression.

In this study, chemoresistance to first-line CHOP-based polychemotherapy was high, even compared to other T-cell lymphomas,[43] let alone that only two thirds of patients had attempted systemic treatment after surgery. Yet, very few patients achieved CR during salvage and all eventually died of treatment toxicity or lymphoma progression. Certainly, there is an unmet medical need to improve treatment. Timely diagnosis and better supportive measures may help to reduce early mortality by improving the PS of MEITL patients and decrease toxicity of first-line therapy in a rapidly growing disease. CHOP-based polychemotherapy was mostly ineffective in our patients; therefore, alternative approaches are urgently needed. Remarkably, five of six patients treated with the ifosfamide, etoposide, epirubicin and methotrexate (IVE-MTX) regimen followed by ASCT proposed for EATL reached CR, but only one survived >24 months.[44] Of note, MEITL and hepatosplenic T-cell lymphoma (HSTL) are both aggressive extranodal chemoresistant diseases, which share biological characteristics.[29,45] Hence, non-CHOP first-line alternative polychemotherapy[46] such as ICE (ifosfamide, carboplatin, etoposide) or IVAC (ifosfamide, etoposide, high-dose cytarabine) followed by systematic consolidation, as recommended by the ESMO guidelines[47] could also be valuable for MEITL. Encouraging results have been reported after first-line auto-HCT[44,48] in both EATL and MEITL.[24] Herein patients receiving first-line HCT had longer OS, but HCT had been offered to young patients achieving CR, hence pre-selecting patients with a better prognosis. Consolidation with allo-HCT has the best potential for relapse prevention in T-cell lymphoma but its use is limited by its toxicity.[49] In MEITL, allo-HCT could be recommended even first-line in eligible patients.

A better understanding of MEITL biology may open the path to innovative treatments beyond chemotherapy and transplantation. Particularly, the aberrant expression of B-cell markers, rare in T-cell lymphoma[50] raises the question of therapies targeting CD20 or CD79, while the lack of CD30 expression discourages the use of brentuximab vedotin. Given the frequent activation of the JAK-STAT pathway the use of JAK inhibitors may be useful.[29] The MEITL-hallmark loss of H3K36 trimethylation, confers high sensitivity to WEE1 kinase inhibitors,[51] such as adavosertib, which is developed in clinical trials for solid tumors and could be evaluated in MEITL.

Disclosures

No conflicts of interest to disclose.

Contributions

LV reviewed morphological data, analyzed data, and wrote the manuscript. DC reviewed and interpreted clinical data and wrote the manuscript. EM analyzed and interpreted sequencing data and wrote the manuscript. BP analyzed data and supervised the statistical analysis. BB supervised FISH and TDS analyses. CB, AD, FL, LCF, FL, AC, PM, SG, BJ, AEY, KL, EB reviewed and interpreted clinical data. ALP, EP, LQM, RB, FRG, CB, RDW, FD, JF, MP, JS performed morphological diagnoses. MHDL contributed with molecular data of cases. VF supported material and data acquisition and collected data. RS reviewed and analyzed genomic data. DV performed research and analyzed the data. PG performed morphological diagnoses, designed research, and analyzed data. OT reviewed and interpreted clinical data, designed research, and wrote the manuscript. LdL performed morphological diagnoses, designed research, obtained funding, analyzed data, and wrote the manuscript.

Acknowledgments

The work developed at the Institute of Pathology of Lausanne, was supported by the histopathology, immunopathology and molecular pathology facilities, and the digital pathology platform of the Institute. The authors would like to thank Dr Nathalie Piazzon and Mr Jean-Daniel Roman for assistance with data management, Mrs Catherine Chapuis for technical assistance, Dr Justine Bouilly and Dr Audrey Letourneau for analysis and interpretation of TDS data and Mrs Cloé Bregnard and Mónica Esteves De Azevedo for performing the FISH studies. They also thank Dr Amedeo Sciarra for his contribution to data coding, Dr Adamantia Kapopoulou and Mr Vimel Rattina for their contribution in whole exome analysis and Mr Venkatesh Kacherla in the preparation of Figure 4 panels. The authors are indebted to Mrs Julien Marquis and Johann Weber from the Lausanne Genomic Technologies Facility, Center for Integrative Genomics of Lausanne University where whole-exome sequencing was performed.

The authors would like to thank Drs Patrick Bruandet and Jacques Akpo-Allavo (Service de Pathologie CH Blois), Drs Florence Bloget and Damienne Declerck (Medipath, Avon), Drs François Lamarche and Caroline Ghighi (ACP, Abbeville), Drs Pierre Boyer and Jean Kapfer (CAP Orléans), Prof Luc Xerri (Service de Pathologie, IPC Marseille) and Dr Thérèse Rousset (Service de Pathologie, CHU Montpellier) for providing tumor material. Dr Olivier Dubroeucq (Institut Jean Godinot, Reims), Dr Bruno Villemagne (CHD Vendée), Dr Emmanuelle Tchernonog (CHU de Montpellier), Dr Sara Bur-

cheri (CH Perpignan), Dr Sophie Rigaudeau (CH de Versailles), Pr Emmanuel Gyan (CHU de Tours), Dr Julie Abraham (CHU de Limoges), Dr Emmanuel Fleck (CH de La Rochelle), Dr Eric Dupont (CH d'Agen), Dr Jean Galtier (CHU de Bordeaux), Dr Thibault Brotelle (CH d'Avignon), Pr Gandhi Damaj (CHU de Caen), Dr Serge Bologna (Centre d'oncologie de Gentilly), Dr Clémentine Sarkozy (Institut Gustave Roussy), Dr Marion Loirat (CH de Saint-Nazaire), Dr Valentin Letailleur (CHU de Nantes), Dr Pierre Englert (Hôpital Erasme, Bruxelles), Romane Muletier (CHU de Clermont-Ferrand), Dr Shota Tsiklauri (CH d'Aubenas), Dr Bernard Drenou (GHR Mulhouse Sud-Alsace), Dr Florian Bouclet (Centre Henri Becquerel, Rouen), Dr Robin Noël (Institut Paoli Calmettes, Marseille), Dr Patrick Mboungou (CH de Boulogne-Sur-Mer), Dr Abdallah Maakaroun (CH de Bourges) and the Hospitals of Dieppe, Mont-de-Marsan, Sud Seine-et-Marne, the Clinique du Saint-Cœur, the Clinique de l'Archette, the Polyclinique du Ternois are acknowledged for providing clinical follow-up.

Funding

This work was supported by the grants KLS-4293-08-2017-R to LDL of the Swiss Cancer Ligue and SNSF – 31BL30_172718 to LDL of the Patholink and the Swiss National Science Foundation.

Data-sharing statement

Original data and protocols will be available to other investigators by request to corresponding author.

References

1. Jaffe ES, Chott A, Ott G, et al. Intestinal T-cell lymphoma. In Swerdlow SH, Campo E, Harris NL editors. WHO Classification of tumours of Haematopoietic and Lymphoid Tissues, revised 4th ed. Lyon, France: IARC Press; 2017. p372-80.
2. Vose J, Armitage J, Weisenburger D, International T-Cell Lymphoma Project. International peripheral T-cell and natural killer/T-cell lymphoma study: pathology findings and clinical outcomes. J Clin Oncol. 2008;26(25):4124-4130.
3. Laurent C, Baron M, Amara N, et al. Impact of expert pathologic review of lymphoma diagnosis: study of patients from the French Lymphopath Network. J Clin Oncol. 2017;35(18):2008-2017.
4. Chott A, Haedicke W, Mosberger I, et al. Most CD56+ intestinal lymphomas are CD8+CD5-T-cell lymphomas of monomorphic small to medium size histology. Am J Pathol. 1998;153(5):1483-1490.
5. Takeshita M, Nakamura S, Kikuma K, et al. Pathological and immunohistological findings and genetic aberrations of intestinal enteropathy-associated T cell lymphoma in Japan. Histopathology. 2011;58(3):395-407.
6. Moffitt AB, Ondrejka SL, McKinney M, et al. Enteropathy-associated T cell lymphoma subtypes are characterized by loss of function of SETD2. J Exp Med. 2017;214(5):1371-1386.
7. Roberti A, Dobay MP, Bisig B, et al. Type II enteropathy-associated T-cell lymphoma features a unique genomic profile with highly recurrent SETD2 alterations. Nat Commun. 2016;7:12602.
8. Delabie J, Holte H, Vose JM, et al. Enteropathy-associated T-cell lymphoma: clinical and histological findings from the international peripheral T-cell lymphoma project. Blood. 2011;118(1):148-155.
9. Tse E, Gill H, Loong F, et al. Type II enteropathy-associated T-cell lymphoma: a multicenter analysis from the Asia Lymphoma Study Group. Am J Hematol. 2012;87(7):663-668.
10. Tan SY, Chuang SS, Tang T, et al. Type II EATL (epitheliotropic intestinal T-cell lymphoma): a neoplasm of intra-epithelial T-cells with predominant CD8αα phenotype. Leukemia. 2013;27(8):1688-1696.
11. Tomita S, Kikuti YY, Carreras J, et al. Genomic and immunohistochemical profiles of enteropathy-associated T-cell lymphoma in Japan. Mod Pathol. 2015;28(10):1286-1296.
12. Sun J, Lu Z, Yang D, Chen J. Primary intestinal T-cell and NK-cell lymphomas: a clinicopathological and molecular study from China focused on type II enteropathy-associated T-cell lymphoma and primary intestinal NK-cell lymphoma. Mod Pathol. 2011;24(7):983-992.
13. Ko YH, Karnan S, Kim KM, et al. Enteropathy-associated T-cell lymphoma-a clinicopathologic and array comparative genomic hybridization study. Hum Pathol. 2010;41(9):1231-1237.
14. Akiyama T, Okino T, Konishi H, et al. CD8+, CD56+ (natural killer-like) T-cell lymphoma involving the small intestine with no evidence of enteropathy: clinicopathology and molecular study of five Japanese patients. Pathol Int. 2008;58(10):626-634.
15. Kikuma K, Yamada K, Nakamura S, et al. Detailed clinicopathological characteristics and possible lymphomagenesis of type II intestinal enteropathy-associated T-cell lymphoma in Japan. Hum Pathol. 2014;45(6):1276-1284.
16. Tan SY, de Leval L. Monomorphic epitheliotropic intestinal T-cell lymphoma. In WHO Classification of Tumors Editorial Board. Digestive system tumours, revised 5th ed. Lyon, France: IARC Press; 2019. p390-2.
17. Chan JK, Chan AC, Cheuk W, et al. Type II enteropathy-associated T-cell lymphoma: a distinct aggressive lymphoma with frequent γδ T-cell receptor expression. Am J Surg Pathol. 2011;35(10):1557-1569.
18. Chen C, Gong Y, Yang Y, et al. Clinicopathological and molecular genomic features of monomorphic epitheliotropic intestinal T-cell lymphoma in the Chinese population: a study of 20 cases. Diagn Pathol. 2021;16(1):114.
19. Huang D, Lim JQ, Cheah DMZ, et al. Whole-genome sequencing reveals potent therapeutic strategy for monomorphic epitheliotropic intestinal T-cell lymphoma. Blood Adv. 2020;4(19):4769-4774.
20. Nairismägi ML, Tan J, Lim JQ, et al. JAK-STAT and G-protein-coupled receptor signaling pathways are frequently altered in epitheliotropic intestinal T-cell lymphoma. Leukemia. 2016;30(6):1311-1319.
21. Küçük C, Jiang B, Hu X, et al. Activating mutations of STAT5B and STAT3 in lymphomas derived from γδ-T or NK cells. Nat Commun. 2015;6:6025.
22. Nicolae A, Xi L, Pham TH, et al. Mutations in the JAK/STAT and RAS signaling pathways are common in intestinal T-cell

lymphomas. Leukemia. 2016;30(11):2245-2247.
23. Tomita S, Kikuti YY, Carreras J, et al. Monomorphic epitheliotropic intestinal T-cell lymphoma in Asia frequently shows SETD2 alterations. Cancers (Basel). 2020;12(12).
24. Yi JH, Lee GW, Do YR, et al. Multicenter retrospective analysis of the clinicopathologic features of monomorphic epitheliotropic intestinal T-cell lymphoma. Ann Hematol. 2019;98(11):2541-2550.
25. de Leval L, Parrens M, Le Bras F, et al. Angioimmunoblastic T-cell lymphoma is the most common T-cell lymphoma in two distinct French information data sets. Haematologica. 2015;100(9):e361-364.
26. Lemonnier F, Dupuis J, Sujobert P, et al. Treatment with 5-azacytidine induces a sustained response in patients with angioimmunoblastic T-cell lymphoma. Blood. 2018;132(21):2305-2309.
27. Morgan EA, Pihan GA, Said JW, et al. Profile of CD103 expression in T-cell neoplasms: immunoreactivity is not restricted to enteropathy-associated T-cell lymphoma. Am J Surg Pathol. 2014;38(11):1557-1570.
28. Paige AJ. Redefining tumour suppressor genes: exceptions to the two-hit hypothesis. Cell Mol Life Sci. 2003;60(10):2147-2163.
29. McKinney M, Moffitt AB, Gaulard P, et al. The genetic basis of hepatosplenic T-cell lymphoma. Cancer Discov. 2017;7(4):369-379.
30. Lemonnier F, Couronné L, Parrens M, et al. Recurrent TET2 mutations in peripheral T-cell lymphomas correlate with TFH-like features and adverse clinical parameters. Blood. 2012;120(7):1466-1469.
31. Couronné L, Bastard C, Bernard OA. TET2 and DNMT3A mutations in human T-cell lymphoma. N Engl J Med. 2012;366(1):95-96.
32. Haddad PA, Dadi N. Clinicopathologic determinants of survival in monomorphic epitheliotropic intestinal T-cell lymphoma (MEITL): analysis of a pooled database. Blood. 2020;136(Suppl 1):S28.
33. Young KH, Weisenburger DD, et al. Mutations in the DNA-binding codons of TP53, which are associated with decreased expression of TRAILreceptor-2, predict for poor survival in diffuse large B-cell lymphoma. Blood. 2007;110(13):4396-4405.
34. Chapuy B, Stewart C, Dunford AJ, et al. Molecular subtypes of diffuse large B cell lymphoma are associated with distinct pathogenic mechanisms and outcomes. Nat Med. 2018;24(5):679-690.
35. Kataoka K, Iwanaga M, Yasunaga JI, et al. Prognostic relevance of integrated genetic profiling in adult T-cell leukemia/lymphoma. Blood. 2018;131(2):215-225.
36. Watatani Y, Sato Y, Miyoshi H, et al. Molecular heterogeneity in peripheral T-cell lymphoma, not otherwise specified revealed by comprehensive genetic profiling. Leukemia. 2019;33(12):2867-2883.
37. Pham HTT, Maurer B, Prchal-Murphy M, et al. STAT5BN642H is a driver mutation for T cell neoplasia. J Clin Invest. 2018;128(1):387-401.
38. Rajala HL, Eldfors S, Kuusanmäki H, et al. Discovery of somatic STAT5b mutations in large granular lymphocytic leukemia. Blood. 2013;121(22):4541-4550.
39. López C, Bergmann AK, Paul U, et al. Genes encoding members of the JAK-STAT pathway or epigenetic regulators are recurrently mutated in T-cell prolymphocytic leukaemia. Br J Haematol. 2016;173(2):265-273.
40. Deleeuw RJ, Zettl A, Klinker E, et al. Whole-genome analysis and HLA genotyping of enteropathy-type T-cell lymphoma reveals 2 distinct lymphoma subtypes. Gastroenterology. 2007;132(5):1902-1911.
41. Deng M, Xu-Monette ZY, Pham LV, et al. Aggressive B-cell Lymphoma with MYC/TP53 dual alterations displays distinct clinicopathobiological features and response to novel targeted agents. Mol Cancer Res. 2021;19(2):249-260.
42. Chapiro E, Lesty C, Gabillaud C, et al. "Double-hit" chronic lymphocytic leukemia: An aggressive subgroup with 17p deletion and 8q24 gain. Am J Hematol. 2018;93(3):375-382.
43. Bachy E, Camus V, Thieblemont C, et al. Romidepsin plus CHOP versus CHOP in patients with previously untreated peripheral T-cell lymphoma: results of the Ro-CHOP phase III study (Conducted by LYSA). J Clin Oncol. 2022;40(3):242-251.
44. Sieniawski M, Angamuthu N, Boyd K, et al. Evaluation of enteropathy-associated T-cell lymphoma comparing standard therapies with a novel regimen including autologous stem cell transplantation. Blood. 2010;115(18):3664-3670.
45. Travert M, Huang Y, de Leval L, et al. Molecular features of hepatosplenic T-cell lymphoma unravels potential novel therapeutic targets. Blood. 2012;119(24):5795-5806.
46. Voss MH, Lunning MA, Maragulia JC, et al. Intensive induction chemotherapy followed by early high-dose therapy and hematopoietic stem cell transplantation results in improved outcome for patients with hepatosplenic T-cell lymphoma: a single institution experience. Clin Lymphoma Myeloma Leuk. 2013;13(1):8-14.
47. d'Amore F, Gaulard P, Trümper L, et al. ESMO Guidelines Committee. Peripheral T-cell lymphomas: ESMO Clinical Practice Guidelines for diagnosis, treatment and follow-up. Ann Oncol. 2015;26 Suppl 5:v108-115.
48. Jantunen E, Boumendil A, Finel H, et al. Autologous stem cell transplantation for enteropathy-associated T-cell lymphoma: a retrospective study by the EBMT. Blood. 2013;121(13):2529-2532.
49. Schmitz N, Truemper L, Bouabdallah K, et al. A randomized phase 3 trial of autologous vs allogeneic transplantation as part of first-line therapy in poor-risk peripheral T-NHL. Blood. 2021;137(19):2646-2656.
50. Blakolmer K, Vesely M, Kummer JA, Jurecka W, Mannhalter C, Chott A. Immunoreactivity of B-cell markers (CD79a, L26) in rare cases of extranodal cytotoxic peripheral T- (NK/T-) cell lymphomas. Mod Pathol. 2000;13(7):766-772.
51. Pfister SX, Markkanen E, Jiang Y, et al. Inhibiting WEE1 selectively kills histone H3K36me3-deficient cancers by dNTP starvation. Cancer Cell. 2015;28(5):557-568